p53 binds more dynamically to response elements that are closer to the consensus sequence

Johannes P. Suwita[1], Elina Ly[2], James A. Goodrich[3]*, and Jennifer F. Kugel[3]*

[1]Faculty of Biology and Preclinical Medicine, University of Regensburg, 93040 Regensburg, Germany

[2]KBI Biopharma, 1450 Infinite Drive, Louisville CO, 80027, USA

[3]Department of Biochemistry, University of Colorado Boulder, 596 UCB, Boulder CO, 80309, USA

*Corresponding authors: jennifer.kugel@colorado.edu, james.goodrich@colorado.edu

Abstract

The transcriptional activator p53 is a tumor suppressor protein that controls cellular pathways important for cell fate decisions, including cell cycle arrest, senescence, and apoptosis. It functions as a tetramer by binding to specific DNA sequences known as response elements (REs) to control transcription via interactions with co-regulatory complexes. Critical for understanding how p53 regulates gene expression is unraveling the fundamental mechanisms by which it binds to REs. Toward this goal we have used an in vitro single molecule fluorescence approach to quantify the dynamic binding of tetrameric p53 to different REs in real time under equilibrium conditions. For each RE tested we measured a single rate constant for association and two rate constants for dissociation, showing two kinetically distinguishable populations of tetrameric/RE complexes. Moreover, p53/DNA interactions were more dynamic as the RE sequence became closer to the consensus sequence. We propose a model in which p53 and its RE consensus sequence evolved to favor dynamic binding.

Introduction

The transcriptional activator and tumor suppressor p53 is one of the most widely studied mammalian proteins. The p53 protein forms a tetramer consisting of four monomers (393 amino acids) that each contain a core DNA binding domain and oligomerization domain flanked by an acidic N-terminal region and an unstructured C-terminal tail[1,2]. p53 tetramers bind DNA at p53 response elements (REs), which are composed of two 10 bp half site sequences separated by 0–13 base pairs[3,4]. The half site consensus sequence is RRRCWWGYYY, where R represents A or G, W represents A or T, and Y represents C or T[3,4]. p53 REs are found throughout mammalian genomes, and p53 binding controls the transcription of genes involved in multiple cellular pathways including stress response pathways and cell cycle control[5,6]. Most of the biochemical and structural studies of p53 have been performed with isolated domains, such as the DNA binding domain. These studies have yielded critical insight into understanding how p53 interacts with DNA, and importantly, how the many mutations in the DNA binding domain that are associated with a variety of cancers impair the function of the protein[7,8]. Indeed, mutations that disrupt the ability of p53 to bind DNA are among the most prevalent found in tumors, underscoring the importance of understanding how this protein interacts with its REs[9–11].

To gain insight into the mechanisms by which p53 binds to DNA, we previously studied full-length human p53 tetramers interacting with the RE from the promoter of the GADD45 gene in real time using in vitro single molecule fluorescence co-localization assays[12]. This enabled us to investigate p53/DNA complexes under equilibrium conditions, which was important for observing binding specificity. In our single molecule

studies p53 tetramers readily bound the GADD45 RE but not a randomized RE, whereas in electrophoretic mobility shift assays we found that p53 bound to a randomized DNA with low nM affinity[12]. The single molecule system also resolves rapid binding and unbinding events. Indeed, we observed that the p53/RE interactions were surprisingly dynamic, with many binding and release events occurring over tens of seconds. Moreover, p53 tetramers dissociated from the native RE with two different rate constants, showing that two kinetically distinguishable populations of p53/DNA complexes exist[12]. Notably, single particle tracking experiments in live cells have also shown that p53 interacts with chromatin with rapid dynamics. In these experiments, two kinetic populations were observed with average residence times of ~3 s and ~0.3 s[13,14].

Rapid interactions with chromatin are not unique to p53. Indeed, live cell single particle tracking studies of many different mammalian transcription factors reveal that in general transcription factor binding is very dynamic[15]. As examples, chromatin residence times have been measured for Sox2, Oct4, cMyc, CTCF, SRF, and steroid receptors; many of these studies report two populations with short (<1s) and somewhat longer (several seconds) residence times[16–20]. The interactions of transcription factors with chromatin that occur on the order of seconds are thought to represent functional interactions with the genome; indeed, studies have shown they correlate with transcriptional activity[13]. While single particle tracking approaches enable measurements of transcription factors dynamically binding chromatin in live cells, they are not able to distinguish binding to a specific RE. Hence, in vitro kinetic measurements are required to distinguish how binding dynamics differ between native REs.

To evaluate the relationship between p53 binding kinetics and the sequence of REs, we determined how natural variation in the p53 RE sequence affects the kinetics with which p53 tetramers associate with and dissociate from DNA. We used an in vitro single molecule fluorescence system to quantify the kinetic parameters of p53 binding to four native REs that differ from the consensus sequence by variable amounts. We found that all REs tested showed a similar mechanism of interaction with p53 tetramers: little evidence of dimer/DNA complexes en route to binding or dissociation, and two populations of tetramer/DNA complexes that dissociate with different kinetics. Unexpectedly, the measured rate constants for association and dissociation were both larger (i.e. more rapid) at REs closest to consensus. Our results support the model that p53 REs evolved such that sites closer to consensus bind p53 tetramers with greater dynamics.

Results

A single molecule system for studying p53 tetramers dynamically binding to DNA

We previously developed a single molecule fluorescence system for studying the binding of tetrameric p53 to DNA using a TIRF (total internal reflection fluorescence) microscope[12]. A key component of this system is fluorescently labeled full length recombinant human p53, which is expressed in insect cells with an N-terminal His tag and a C-terminal SNAP tag for labeling (p53-SNAP). After purification the p53-SNAP is labeled with AlexaFluor647 (AF647-p53). AF647-p53 is fully active for DNA binding when compared to wild-type p53; moreover, the dye conjugation is near 100% as assessed by LC MS/MS with ~70% of the dyes being photoactive[12].

An overview of the single molecule system used to study DNA binding by AF647-p53 is shown in Figure 1A. First, AF647-labeled DNA containing a p53 RE is immobilized on the surface of a slide chamber via a biotin tag. We then image the immobilized AF647 DNA molecules in 4 regions to register their locations using a TIRF microscope (i.e. DNA-only movie). AF647-p53 is then flowed into the chamber and we image the same four regions over time to monitor p53 binding events (i.e. DNA+p53 movie). For each region, spots of AF647 emission from the DNA+p53 movie are co-localized with spots of AF647 emission from the DNA-only movie. To identify and quantify p53 tetramer binding and dissociation events, the fluorescence emission is quantified over time for each spot pair. The fluorescence intensity of the AF647 emission from a given spot in the DNA-only movie is used to obtain a baseline intensity for a single red dye at that position on the surface. Using this baseline, the number of dye molecules associated with each AF647-p53 binding and dissociation event is calculated, which yields the oligomeric state of p53 for each binding and dissociation event. Therefore the dynamic interaction of p53 tetramers with a RE can be studied in real time under equilibrium conditions.

Figure 1B shows representative data for the dynamic binding of p53 at a single DNA molecule containing the PUMA RE over a 575 s movie. The plot of fluorescence intensity over time shows that at the beginning of the movie tetrameric p53 is bound to the DNA, then at ~65 s this molecule of p53 dissociates from the DNA. Throughout the remainder of the movie, four other p53 tetramers bound and dissociated from this same DNA molecule. Each change in fluorescence intensity (i.e. each increase or decrease) in the plot was approximately 4 times the intensity of the DNA molecule, consistent with

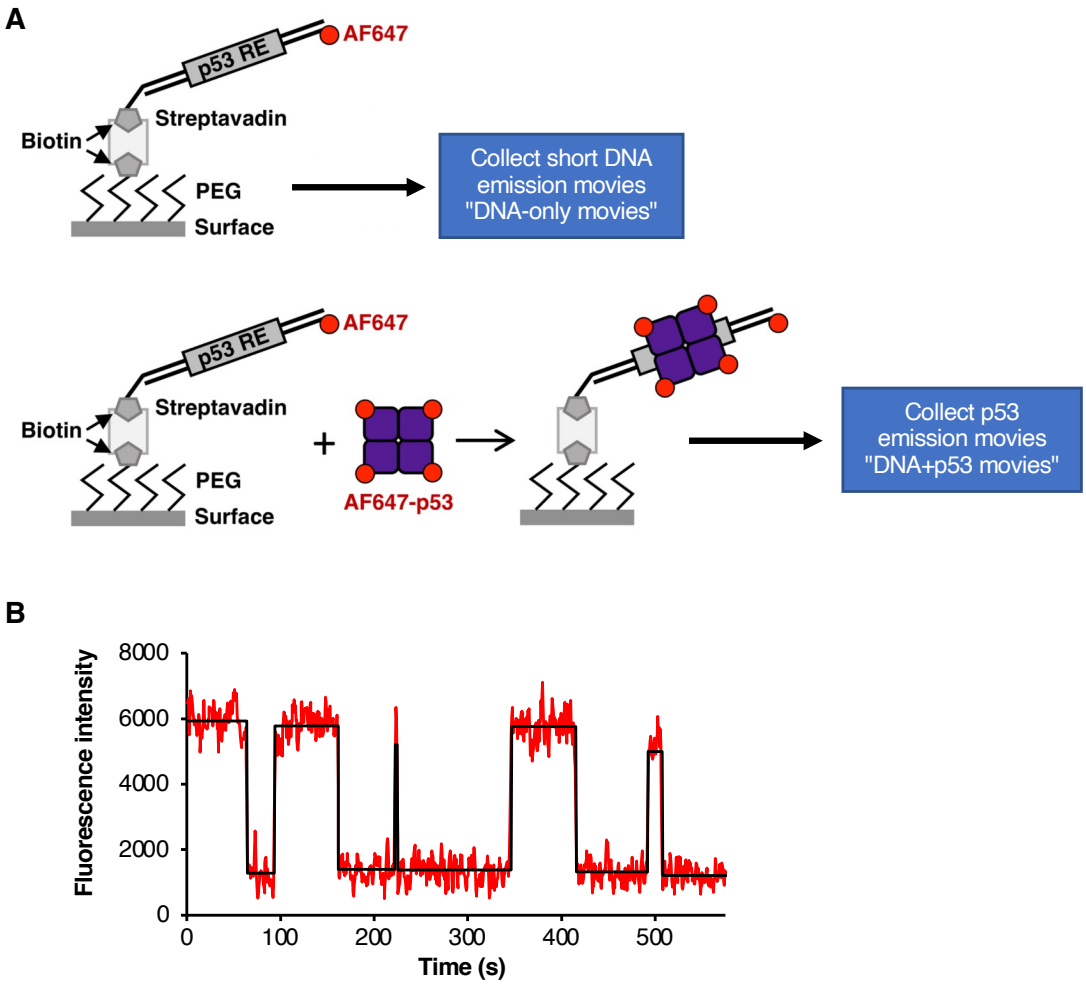

Figure 1. A single molecule fluorescence assay to study dynamic DNA binding by tetrameric p53. (**A**) Illustration of the single molecule assay used. Red emission movies were collected of biotinylated AF647 labeled DNA immobilized on the streptavidin derivatized surface. A second red emission movie (DNA + p53 movie) was collected over the same region after AF647-p53 was flowed into the slide chamber. p53 biding events on immobilized DNA were identified by co-localization of molecules in the DNA only data and the DNA + p53 data. Emission intensity traces over time were generated for each spot pair, and were used to calculate the base intensity value for a single dye on the DNA and the number of dyes (i.e. oligomeric state) of p53 bound to DNA. Figure is adapted from[12]. (**B**) Representative AF647 emission data from a single DNA molecule with five tetrameric p53 binding events. For this movie, emission data were collected every 600 ms for 590 frames. The immobilized DNA contained the PUMA RE, and the p53 tetramer concentration was 0.24 nM, assuming all monomers were in tetramers. For purposes of display, the signals were smoothed by averaging three adjacent time frames.

each event involving binding or dissociation of tetrameric p53. We focused our studies on tetrameric binding and dissociation events, which showed a change of three or four dye intensity units, which accounts for the fact that only ~70% of the dye molecules are fluorescently active (i.e. some tetramers have only three active dyes). Limiting our analysis in this manner also ensured that dissociation events were not due to photobleaching or photoblinking, which would not occur simultaneously for the three or four active AF647 dyes.

p53 tetramers show concerted binding and dissociation on native REs

We were interested in determining how natural variability in the sequence of the p53 RE affects the mechanism and dynamics of binding by p53 tetramers. To study this, we chose four native REs that diverge from the p53 RE consensus sequence at one, two, or three positions; all the REs had no additional basepairs between the two half sites (Figure 2A). Each of the native REs has the most highly conserved two base pairs in each half site (the C/G at position 4 and the G/C at position 7). The GADD45 RE, which we previously studied, is most similar to consensus, differing at only one position. The p21 and MDM2 REs differ from consensus at two positions, and the PUMA RE differs from consensus at three positions. We also designed a partially randomized 20 bp DNA with only half of the basepairs matching the p53 RE consensus sequence.

We performed multiple single molecule experiments with each DNA separately immobilized, using 0.24 nM p53 (maximal tetrameric concentration). For each DNA we quantified the number of tetrameric DNA binding and dissociation events (i.e. those showing three or four dye units of intensity change). For each of the REs we obtained

A

```
Consensus:  5'-RRRCWWGYYYRRRCWWGYYY-3'
GADD45:     5'-GAACATGTCTAAGCATGCTg-3'
p21:        5'-GAACATGTCCcAACATGTTg-3'
MDM2:       5'-GAACgTGTCTGAACTTGaCC-3'
PUMA:       5'-GGACAAGTCaGGACTTGCag-3'
Randomized: 5'-tAAtcgGgTaGGGgcTGaCa-3'
```

B

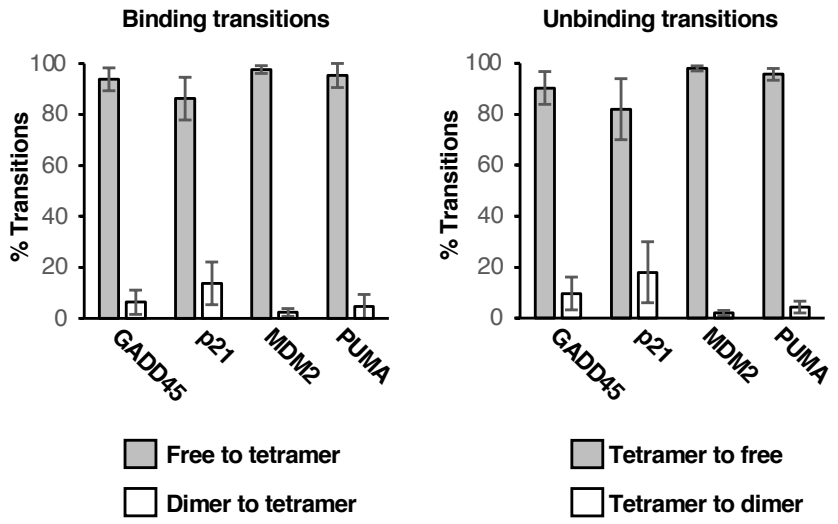

Figure 2. p53 tetramers dynamically associate with four native REs. (**A**) The four native RE sequences and randomized sequence used in the single molecule experiments in comparison to the p53 RE consensus sequence. Positions that are not consensus are shown in red, lowercase letters. R represents A or G, W represents A or T, and Y represents C or T. (**B**) Tetrameric p53 does not go through a dimer intermediate en route to binding to or dissociating from each of the four REs. Plotted is the percentage of transitions that were tetramers (e.g. gain/loss of 3 or 4 dyes) or dimers (e.g. gain/loss of 2 dyes when transitioning to or from a tetrameric p53/DNA complex). The errors are the standard deviations of the measurements, with n = 6, 4, 3, and 3 for the GADD45, p21, MDM2, and PUMA elements, respectively. For each RE, the eight pairwise comparisons of tetramer/free transitions (gray bars) to dimer/tetramer transitions (white bars) have a p values < 0.0003 using an unpaired two-sided t test. For each type of transition, the pairwise comparisons between REs showed no significant differences, all p values were > 0.05 using an unpaired two-sided t test.

hundreds of binding and unbinding events. For each event we evaluated whether binding or dissociation proceeded through a pathway in which an intermediate dimer/ DNA complex was detected. To do so we asked if binding and dissociation events involved the gain or loss of two dye molecules en route to the final bound or unbound state. As shown in the bar plots in Figure 2B, on each of the four REs, the vast majority of the events showed tetrameric binding and dissociation that did not proceed through an intermediate (gray bars), consistent with what we observed in our previous experiments with the GADD45 RE[12]. Moreover, there is no significant difference between the REs regarding the percentage of each type of transition (i.e. tetramer/free or tetramer/dimer), showing that p53 binds and releases each RE via the same pathway. We also performed controls with no DNA on the surface and with the immobilized partially randomized DNA (sequence shown in Figure 2A). In these two conditions we observed very few (maximum of 10) binding and unbinding events compared to hundreds on the REs. Hence p53 tetramers did not dynamically bind to the slide surface in general or to a DNA with a sequence that is far away from consensus.

p53 tetramers bind faster to REs that are closer to the consensus sequence

We next asked whether there were differences in the kinetics of binding and release with the four different REs. We began by studying the association of p53 tetramers with the four REs. To do so we measured hundreds of unbound dwell times (i.e. the time between two binding events) on each DNA to determine observed rate constants for association. For each RE, the unbound dwell times were plotted as cumulative sums and fit with a single exponential equation, yielding the observed rate

constants ($k_{on(obs)}$, s^{-1}) shown in Table 1, along with 95% confidence intervals of the curve fits. The unbound dwell time data and curve fits for p53 tetramers binding the four REs are shown in Figures 3A-3D. Plots of the residuals for fitting each of the data sets to a single exponential equation are shown in Supplemental Figure 1. The rate constants span approximately a 3-fold range, from 0.0169 s^{-1} for the PUMA RE to 0.052 s^{-1} for the GADD45 RE. Values for a second order rate constant (k_{on}) were calculated using the concentration of tetrameric p53, and range from 7.1×10^7 $M^{-1}s^{-1}$ for the PUMA RE to 2.2×10^8 $M^{-1}s^{-1}$ for the GADD45 RE. In general, the observed rate constant for association increased as the RE sequence moved toward the consensus sequence. Therefore at a given concentration of p53, REs closest to consensus will be bound faster by p53 than those that are further from the consensus sequence.

p53 tetramers dissociate faster from REs that are closer to the consensus sequence

To determine observed rate constants for dissociation, we measured hundreds of bound dwell times (i.e. the length of time tetrameric p53 remained bound to a single DNA) with the four REs. We found, however, that the bound dwell times for each of the REs plotted as cumulative sums did not fit well to a single exponential equation (see Supplemental Figures 2 and 3 for the single exponential curve fits of the data and the residuals plots). For each of the four REs, the fit of the bound dwell time data improved substantially when using a double exponential equation (Figures 4A-D, with the residuals plots shown in Supplemental Figure 3). This yielded two rate constants (k_{off1} and k_{off2}, s^{-1}), which are shown in Table 1, along with 95% confidence intervals and the percentage of complexes that dissociated with each rate constant. This is indicative of

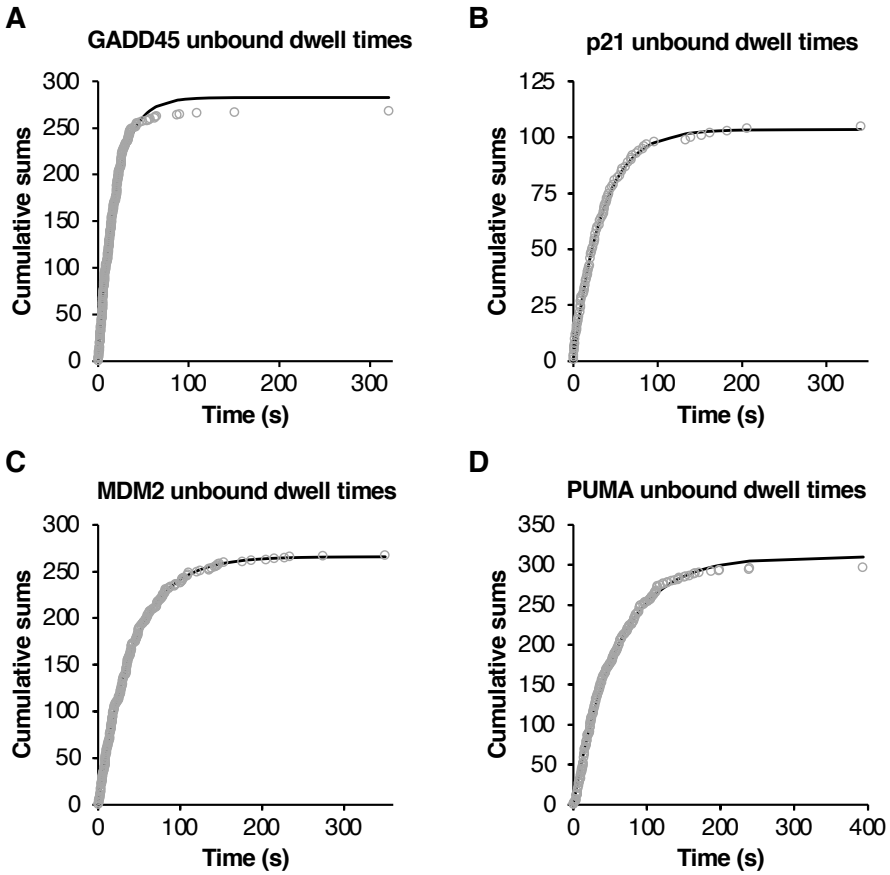

Figure 3. Under equilibrium conditions tetrameric p53 dynamically associated with each of the four REs. Each of the data sets were plotted as cumulative sums over time and fit with a single exponential equation. (**A**) Unbound dwell times (268) obtained with the GADD45 RE were plotted. The rate constant from the single exponential fit is 0.052 s^{-1} with 95% confidence interval of 0.051-0.054 s^{-1}. (**B**) Unbound dwell times (105) obtained with the p21 RE were plotted. The rate constant from the single exponential fit is 0.030 s^{-1} with 95% confidence interval of 0.029-0.031 s^{-1}. (**C**) Unbound dwell times (268) obtained with the MDM2 RE were plotted. The rate constant from the single exponential fit is 0.0237 s^{-1} with 95% confidence interval of 0.0235-0.0240 s^{-1}. (**D**) Unbound dwell times (297) obtained with the PUMA RE were plotted. The rate constant from the single exponential fit is 0.0169 s^{-1} with 95% confidence interval of 0.0166-0.0173 s^{-1}.

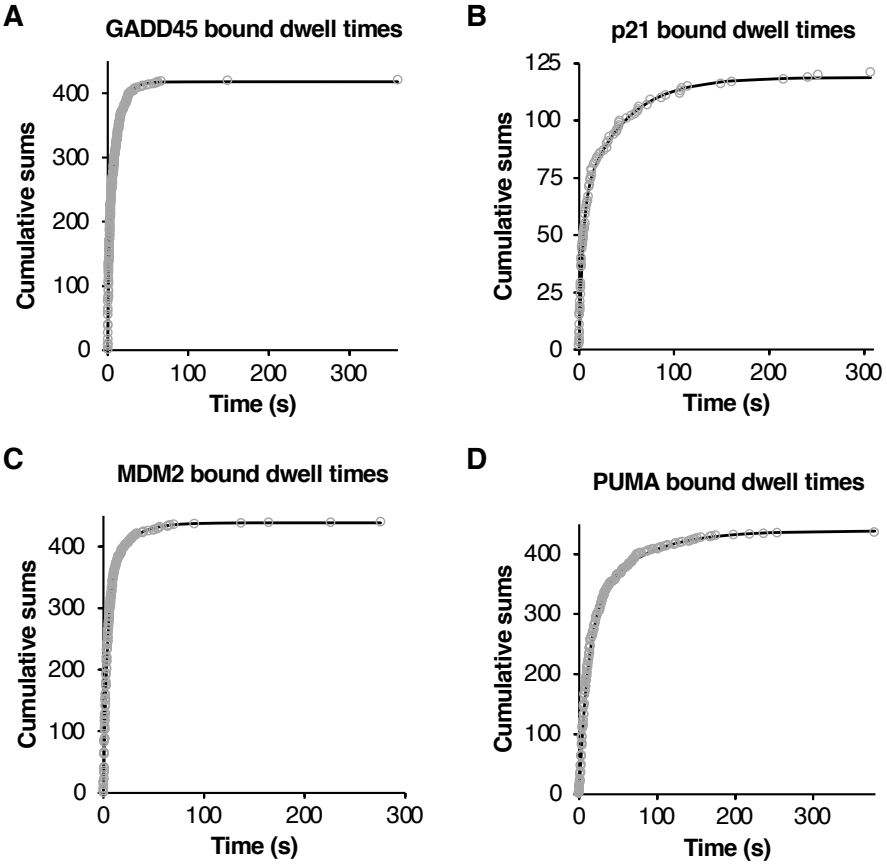

Figure 4. Under equilibrium conditions tetrameric p53 dissociated from each of the four REs in two kinetically distinct steps. Each of the data sets were plotted as cumulative sums over time and fit with a double exponential equation. The rate constants, 95% confidence intervals, and percentage of events contributing to each rate constant are shown in Table 1. (**A**) Bound dwell times (421) obtained with the GADD45 RE were plotted. The rate constants from the double exponential fit are 0.75 s^{-1} and 0.097 s^{-1}. (**B**) Bound dwell times (121) obtained with the p21 RE were plotted. The rate constants from the double exponential fit are 0.27 s^{-1} and 0.023 s^{-1}. (**C**) Bound dwell times (441) obtained with the MDM2 RE were plotted. The rate constants from the double exponential fit are 0.26 s^{-1} and 0.049 s^{-1}. (**D**) Bound dwell times (436) obtained with the PUMA RE were plotted. The rate constants from the double exponential fit are 0.089 s^{-1} and 0.016 s^{-1}.

two kinetically distinct complexes existing on each RE, consistent with our earlier findings on the GADD45 RE[12]. For a given RE, the difference between the upper and lower rate constants for dissociation ranged from 5.3-fold for the MDM2 RE to 11.8-fold for the p21 RE. In general, the rate constants for dissociation increased as the RE sequence moved toward the consensus sequence, indicating that p53 tetramers dissociate faster from REs closest to consensus than those that are further from the consensus sequence.

We estimated the binding affinities for p53 tetramers at each of the four REs by we calculating apparent K_D values (Table 1); our calculations were made assuming all p53 in the reaction was tetrameric, hence the apparent K_D values are upper limits. For the apparent K_D values calculated using the larger dissociation rate constants there is an inverse correlation between the affinity and similarity to consensus (i.e. the RE that is closest to consensus has the lowest apparent affinity). There is no obvious correlation between affinity and consensus for the apparent K_D values calculated using the smaller dissociation rate constants. Together our kinetic data show that rapid on/off binding dynamics correlates best with similarity to consensus sequence.

Discussion

We studied the dynamic binding of p53 tetramers to native REs with variable amounts of divergence from the p53 RE consensus sequence using single molecule fluorescence microscopy. We found that the association of p53 tetramers to each of the REs occurred in a single kinetic step, whereas dissociation from each of the REs occurred with two kinetically distinct events. The rate constants governing the

association and dissociation of p53 tetramers to the different REs varied over an 8-fold range. Unexpectedly, the rates of association and dissociation increased as the sequence of the REs became closer to consensus, supporting a model in which p53 and its RE consensus sequence evolved to favor dynamic binding.

To illustrate that dynamic binding increases as the REs become closer to consensus, plots of the measured rate constants versus the similarity to the p53 RE consensus sequence are shown in Figure 5A. For each of the three sets of rate constants (one association and two dissociation), the general trend shows that the rate constant increases (i.e. binding and unbinding become faster) as the REs become more similar to the consensus sequence. It is not surprising that the rate constant for association increased as the sequence became more similar to consensus, since this could lead to increased affinity. However, our observation that the rate constants for dissociation generally increased as REs become more similar to consensus is unexpected since increased rates of dissociation can lead to decreased affinity. As shown in Table 1, the calculated apparent K_D values trend up as the REs become more similar to consensus, reflecting reduced affinity. Indeed, the largest calculated K_D values (i.e. lowest affinity) for each of the two populations of complexes are both associated with the GADD45 RE, which is the most similar to consensus. This trend in apparent affinity is being driven by the more rapid dissociation that occurs as the REs move toward consensus. Hence, we conclude that for the four native p53 REs we studied, similarity to consensus correlates with overall increased p53 binding dynamics, and not with increased binding affinity, as might be expected.

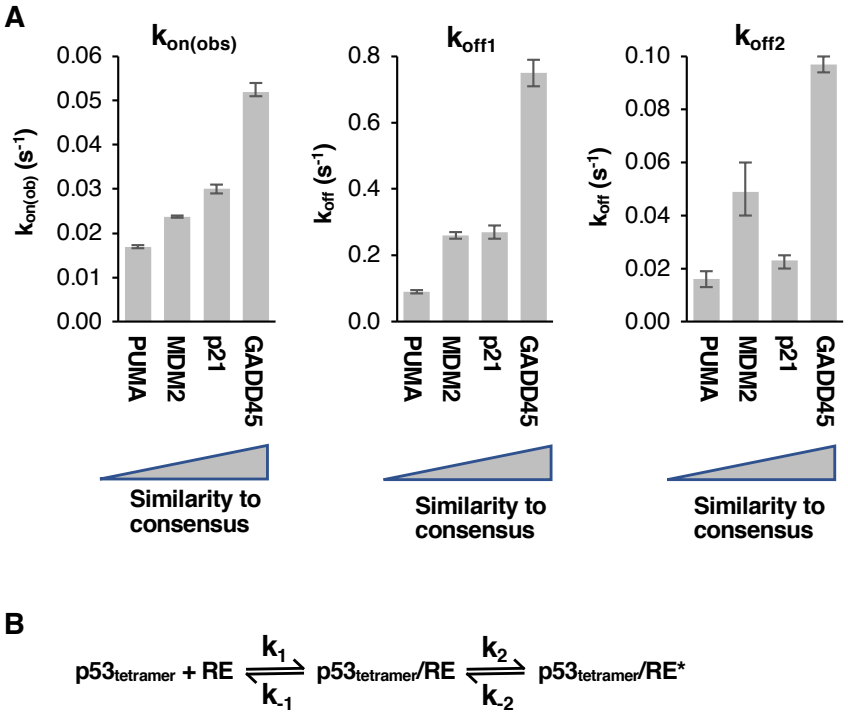

Figure 5. The dynamics of p53 tetramers interacting with p53 REs increases as DNA sequence becomes more similar to the consensus sequence. (**A**) The three measured rate constants are plotted for the four REs, which increase in similarity to consensus from left to right. The errors are 95% confidence intervals. (**B**) Kinetic model for the binding of p53 tetramers to an RE.

The model that p53/RE interactions are governed by dynamics is consistent with other work. Prior structural studies of p53/DNA complexes together with kinetic measurements led to the proposal that p53 relies on differences in dissociation rates rather than differences in affinity to distinguish and recognize specific REs from random DNA[21]. In other words, differences in the kinetic stability (i.e. rate of dissociation) between p53 and different DNAs facilitates binding sequence specificity. The unstructured C-terminal domain of p53 has been shown to facilitate p53 binding to REs that are more divergent from the consensus sequence[22]. It is proposed the C-terminal domain does so by impacting the kinetic stability of complexes[22]. Additional studies will be required to fully explore the relationship between binding dynamics and sequence selectivity for p53, as well as determine if transcription factors other than p53 have evolved to favor dynamic interactions with their consensus sequences.

Our data show that tetrameric p53/DNA complexes that form at four different REs exist in two kinetic populations. Specifically, the bound dwell time data yielded two dissociation rate constants for p53 tetramer/DNA complexes. This is consistent with our previous finding for the GADD45 RE[12], suggesting a general kinetic mechanism for how tetrameric p53 associates with DNA. We favor a model in which the two kinetically distinct complexes result from a linear pathway, as shown in Figure 5B. In this model a p53 tetramer initially binds to the RE in a relatively unstable complex and then undergoes a conformational change to form a more stable complex. We have proposed that the initial recognition and binding event primarily involves one half site, which is followed by interactions with the second half site that stabilize the p53/DNA complex[12]. It is possible that the two kinetically distinct populations we observe result from a

branched pathway rather than a linear pathway. However, it is unlikely that the two independent association interactions in a branched pathway would have identical rate constants at each of the four REs. Moreover, other studies also support a two-step binding mechanism that involves an initial binding interaction followed by a conformational change[21,23–25]. It has been proposed this "induced-fit" mechanism of binding suggests the selectivity of the RE bound is more dependent on the off-rate kinetics, rather than on the on-rate kinetics[25], consistent with our observations. Moreover, as REs become closer to consensus we observe that the distribution of p53 tetramer/DNA complexes shifts toward the more stable of the two conformations (i.e. the percentage of complexes that exhibit the longer half time increases).

The kinetic measurements we report here for p53/DNA complexes in vitro are consistent with measurements made for p53/chromatin interactions in live cells[13,14], with interactions lasting only seconds in both cases. This kinetic profile for a transcription factor is not unique to p53. Rapid on/off kinetics for transcription factors binding to chromatin in live cells has been widely observed in single particle tracking experiments, with time scales similar to what we measured here[15]. Hence single molecule approaches that enable real-time kinetic measurements (in cells and in vitro) have led to an evolution of the traditional regulatory models of stable binding between transcription factors and their REs. Future in vitro single molecule measurements and live cell imaging can be used to further refine dynamic models for transcriptional control.

Methods

DNA constructs and AF647-p53

Oligonucleotides were ordered HPLC purified from Integrated DNA Technologies. All forward oligonucleotides had a 5′ biotin tag attached to a 24 nt single stranded linker:

5′-CGCGTTCATGGTAGAGTCGTGGAC-3′. All reverse oligonucleotides had a 5′ AF647 dye. The sequences of the oligonucleotides were:

GADD45 forward, 5′-TAGAGCGAACATGTCTAAGCATGCTGGCGTCG-3′;

GADD45 reverse, 5′-CGACGCCAGCATGCTTAGACATGTTCGCTCTA-3′;

p21 forward, 5′-TAGAGCGAACATGTCCCAACATGTTGGCGTCG-3′;

p21 reverse, 5′-CGACGCCAACATGTTGGGACATGTTCGCTCTA-3′;

MDM2 forward, 5′-TAGAGCGGTCAAGTTCAGACACGTTCGCGTCG-3′;

MDM2 reverse, 5′-CGACGCGAACGTGTCTGAACTTGACCGCTCTA-3′

PUMA forward, 5′-TAGAGCCTGCAAGTCCTGACTTGTCCGCGTCG-3′;

PUMA reverse, 5’-CGACGCGGACAAGTCAGGACTTGCAGGCTCTA-3′;

Randomized forward, 5′-CGTTCCTAATCGGGTAGGGGCTGACACGAATA-3′;

Randomized reverse, 5′-TATTCGTGTCAGCCCCTACCCGATTAGGAACG-3′.

Forward and reverse oligonucleotides were annealed in 1X annealing buffer (20 mM Tris pH 7.9, 2 mM $MgCl_2$, 50 mM KCl), with 4 μM reverse oligo and 1 μM forward oligo by incubating at 95 °C for 10 min followed by slow cooling to room temperature. Annealed oligos were gel purified after resolving on a 7% native polyacrylamide gel containing 0.5X TBE. The gel was stained (0.01% SYBR® Gold, 0.5X TBE) and the desired band was cut out and transferred to a 1.5 mL reaction tube. 380 μL of TE Low

(10 mM Tris pH 7.9, 0.1 mM EDTA) and 20 μL 1 M KCl were added to the tube, the gel piece was crushed, and the tube was nutated over night at 4 °C. The gel pieces were pelleted via centrifugation and the supernatant was ethanol precipitated.

AF647-p53 was made as previously described[12]. Briefly, full length human p53 containing an N-terminal His tag and a C-terminal SNAP tag was expressed in SF9 insect cells using a recombinant baculovirus. The protein was purified from cellular extracts using HisPur Ni–NTA resin (Thermo Scientific). The purified protein was labeled with SNAP-Surface Alexa Fluor647 dye (New England Biolabs). The fractional dye labeling and DNA binding activity were assessed as previously described[12].

Single molecule binding assays

Microscope slides and coverslips were prepared as described[26]. In brief, slides and coverslips were cleaned in a water bath sonicator in multiple steps with 1% alconox, 100% ethanol, 1 M KOH and 100% methanol. Then, they were functionalized with aminosilane, PEGylated with biotin-PEG/mPEG, and the flow chambers were assembled. All buffers and solutions needed for the assays were prepared as described[12,26].

To perform the single molecule binding assays, the flow chamber was washed twice with 200 μL ddH_2O then twice with 200 μL 1X buffer (25 mM Tris pH 7.9, 50 mM KCl, 5 mM $MgCl_2$, 10% glycerol, 0.05 mg/mL BSA, 1 mM DTT, 0.1% NP-40). A streptavidin solution (50 μL of 0.2 mg/mL streptavidin, 0.8 mg/mL BSA diluted in 1X buffer) was flowed into the chamber. After an incubation of 5 min, the unbound streptavidin was removed by washing twice with 200 μL 1X buffer. Next, 100 μL of

10 pM DNA in 1X buffer was flowed into the chamber and incubated for 10 min. Unbound DNA was removed by washing twice with 200 μL 1X buffer. Then, 100 μL of imaging buffer (1.02 mg/mL glucose oxidase, 0.04 mg/mL catalase, 0.83% D-glucose, 3.04 mM Trolox diluted in 1X buffer) was flowed in and DNA-only emission movies were collected over four regions of the slide using a piezo nanopositioning stage. The flow chamber was washed again with 200 μL of 1X buffer. AF647-p53 (0.24 nM AF647-p53 (tetrameric concentration) diluted in imaging buffer containing 1.25 mg/mL BSA) was flowed into the chamber and DNA+p53 emission movies were collected over the same four regions.

Emission movies were collected with an objective based TIRF microscope (1.49 NA immersion objective, Nikon TE-2000U microscope) and an Andor iXon Life 897 EMCCD camera using the NIS Elements Software. AF647 fluorophores were excited with a 635 nm laser. The laser intensity was set between 115 mA and 125 mA. DNA+p53 movies were collected for 1000 frames (frame rate of 60 ms or 600 ms) or for 2000 frames (frame rate of 200 ms); the corresponding DNA-only movies were collected for 100 frames. A neutral density filter was used to reduce photobleaching during long measurements with an exposure of 200 ms or 600 ms.

Analysis of single molecule data

Emission movies of DNA+p53 were analyzed as described using in-house software written in IDL[12]. Briefly, spots in the DNA-only movie and the DNA+p53 movie from the same region of a slide were computationally colocalized. First, fluorescent spots with an intensity within the user-defined range were identified in the summed

image of each movie individually. Then, if the distance between a spot in the DNA-only movie and a spot in the DNA+p53 movie was ≤ 1-3 pixels, the two spots were considered a potential spot pair. Each potential spot pair was manually visualized and evaluated. A spot pair was rejected if, for example, two spots in close proximity were identified as one spot.

States (unbound and bound DNA) and state changes were computationally determined from the emission intensity over time of a spot and manually visualized and reviewed. For each spot, the emission intensity in the DNA-only movie was defined as the intensity of one AF647 dye (1N). This value was used to classify the oligomeric state of p53 for bound states at that spot in the DNA+p53 movie. For example, the state of the spot in the DNA+p53 movie was classified as unbound if the emission intensity was 1N, dimer-bound if it was 3N, and tetramer-bound if it was 4N or 5N. The number of states, binding/unbinding transitions, and dwell times were compiled across each region and for multiple slides (biological replicates) for each RE. To determine rate constants, bound dwell times (unbound to tetramer-bound to unbound) and unbound dwell times (tetramer-bound to unbound to tetramer-bound) from individual replicates were combined and plotted as cumulative sums. Single and double exponential fits were generated using Solver in Microsoft Excel. Half times for binding and unbinding were calculated from the equation for a first-order reaction: $t_{1/2} = \ln 2/k$. 95% confidence intervals were obtained in GraphPad Prism 8.

References

1. Joerger, A. C. & Fersht, A. R. The tumor suppressor p53: from structures to drug discovery. *Cold Spring Harb Perspect Biol* **2**, a000919 (2010).
2. Joerger, A. C. & Fersht, A. R. The p53 Pathway: Origins, Inactivation in Cancer, and Emerging Therapeutic Approaches. *Annu Rev Biochem* **85**, 375-404 (2016).
3. Brázda, V. & Fojta, M. The Rich World of p53 DNA Binding Targets: The Role of DNA Structure. *Int J Mol Sci* **20**, E5605 (2019).
4. el-Deiry, W. S., Kern, S. E., Pietenpol, J. A., Kinzler, K. W. & Vogelstein, B. Definition of a consensus binding site for p53. *Nat Genet* **1**, 45-49 (1992).
5. Vousden, K. H. & Lane, D. P. p53 in health and disease. *Nat Rev Mol Cell Biol* **8**, 275-283 (2007).
6. Vousden, K. H. & Prives, C. Blinded by the Light: The Growing Complexity of p53. *Cell* **137**, 413-431 (2009).
7. Muller, P. A. & Vousden, K. H. p53 mutations in cancer. *Nat Cell Biol* **15**, 2-8 (2013).
8. Mantovani, F., Collavin, L. & Del Sal, G. Mutant p53 as a guardian of the cancer cell. *Cell Death Differ* **26**, 199-212 (2019).
9. Sigal, A. & Rotter, V. Oncogenic mutations of the p53 tumor suppressor: the demons of the guardian of the genome. *Cancer Res* **60**, 6788-6793 (2000).
10. Joerger, A. C. & Fersht, A. R. Structural biology of the tumor suppressor p53 and cancer-associated mutants. *Adv Cancer Res* **97**, 1-23 (2007).
11. Hainaut, P. & Pfeifer, G. P. Somatic TP53 Mutations in the Era of Genome Sequencing. *Cold Spring Harb Perspect Med* **6**, a026179 (2016).

12. Ly, E., Kugel, J. F. & Goodrich, J. A. Single molecule studies reveal that p53 tetramers dynamically bind response elements containing one or two half sites. *Sci Rep* **10**, 16176 (2020).

13. Loffreda, A. et al. Live-cell p53 single-molecule binding is modulated by C-terminal acetylation and correlates with transcriptional activity. *Nat Commun* **8**, 313 (2017).

14. Morisaki, T., Müller, W. G., Golob, N., Mazza, D. & McNally, J. G. Single-molecule analysis of transcription factor binding at transcription sites in live cells. *Nat Commun* **5**, 4456 (2014).

15. Wang, Z. & Deng, W. Dynamic transcription regulation at the single-molecule level. *Dev Biol* **482**, 67-81 (2022).

16. Chen, J. et al. Single-molecule dynamics of enhanceosome assembly in embryonic stem cells. *Cell* **156**, 1274-1285 (2014).

17. Hipp, L. et al. Single-molecule imaging of the transcription factor SRF reveals prolonged chromatin-binding kinetics upon cell stimulation. *Proc Natl Acad Sci U S A* **116**, 880-889 (2019).

18. Hansen, A. S., Amitai, A., Cattoglio, C., Tjian, R. & Darzacq, X. Guided nuclear exploration increases CTCF target search efficiency. *Nat Chem Biol* **16**, 257-266 (2020).

19. Izeddin, I. et al. Single-molecule tracking in live cells reveals distinct target-search strategies of transcription factors in the nucleus. *Elife* **3**, (2014).

20. Paakinaho, V. et al. Single-molecule analysis of steroid receptor and cofactor action in living cells. *Nat Commun* **8**, 15896 (2017).

21. Petty, T. J. et al. An induced fit mechanism regulates p53 DNA binding kinetics to confer sequence specificity. *EMBO J* **30**, 2167-2176 (2011).

22. Laptenko, O. et al. The p53 C terminus controls site-specific DNA binding and promotes structural changes within the central DNA binding domain. *Mol Cell* **57**, 1034-1046 (2015).

23. Emamzadah, S., Tropia, L., Vincenti, I., Falquet, B. & Halazonetis, T. D. Reversal of the DNA-binding-induced loop L1 conformational switch in an engineered human p53 protein. *J Mol Biol* **426**, 936-944 (2014).

24. D'Abramo, M. et al. The p53 tetramer shows an induced-fit interaction of the C-terminal domain with the DNA-binding domain. *Oncogene* **35**, 3272-3281 (2016).

25. Chillemi, G. et al. Structural Evolution and Dynamics of the p53 Proteins. *Cold Spring Harb Perspect Med* **7**, a028308 (2017).

26. Ly, E., Goodrich, J. A. & Kugel, J. F. Monitoring transcriptional activity by RNA polymerase II in vitro using single molecule co-localization. *Methods* **159-160**, 45-50 (2019).

Acknowledgements

This research was funded by grant MCB-1817442 from the National Science Foundation. J.P.S. was supported by the Max Weber-Programm scholarship from Elitenetzwerk Bayern and C. H. Boehringer Sohn AG & Co. KG, Ingelheim, Germany. E.L. was supported by NSF Graduate Research Fellowship Program award DGE1144083.

Author contributions

J.P.S., J.A.G., and J.F.K. conceived and designed the project. E.L. cloned, purified, and fluorescently labeled the protein. J.P.S. acquired data and analyzed data. J.A.G. wrote software for data analysis. J.A.G, J.F.K. and J.P.S. wrote the manuscript. All authors contributed to manuscript revision, and have read and approved the final version.

Competing interests

The authors declare no competing interests.

Data availability

The raw single molecule data, dwell time plots, and IDL analysis software used in this study are publicly available on the Open Science Framework platform.

Figure Legends

Figure 1. A single molecule fluorescence assay to study dynamic DNA binding by tetrameric p53. (**A**) Illustration of the single molecule assay used. Red emission movies were collected of biotinylated AF647 labeled DNA immobilized on the streptavidin derivatized surface. A second red emission movie (DNA + p53 movie) was collected over the same region after AF647-p53 was flowed into the slide chamber. p53 biding events on immobilized DNA were identified by co-localization of molecules in the DNA only data and the DNA + p53 data. Emission intensity traces over time were generated for each spot pair, and were used to calculate the base intensity value for a single dye on the DNA and the number of dyes (i.e. oligomeric state) of p53 bound to DNA. Figure

is adapted from[12]. (**B**) Representative AF647 emission data from a single DNA molecule with five tetrameric p53 binding events. For this movie, emission data were collected every 600 ms for 590 frames. The immobilized DNA contained the PUMA RE, and the p53 tetramer concentration was 0.24 nM, assuming all monomers were in tetramers. For purposes of display, the signals were smoothed by averaging three adjacent time frames.

Figure 2. p53 tetramers dynamically associate with four native REs. (**A**) The four native RE sequences and randomized sequence used in the single molecule experiments in comparison to the p53 RE consensus sequence. Positions that are not consensus are shown in red, lowercase letters. R represents A or G, W represents A or T, and Y represents C or T. (**B**) Tetrameric p53 does not go through a dimer intermediate en route to binding to or dissociating from each of the four REs. Plotted is the percentage of transitions that were tetramers (e.g. gain/loss of 3 or 4 dyes) or dimers (e.g. gain/loss of 2 dyes when transitioning to or from a tetrameric p53/DNA complex). The errors are the standard deviations of the measurements, with n = 6, 4, 3, and 3 for the GADD45, p21, MDM2, and PUMA elements, respectively. For each RE, the eight pairwise comparisons of tetramer/free transitions (gray bars) to dimer/tetramer transitions (white bars) have a p values < 0.0003 using an unpaired two-sided t test. For each type of transition, the pairwise comparisons between REs showed no significant differences, all p values were > 0.05 using an unpaired two-sided t test.

Figure 3. Under equilibrium conditions tetrameric p53 dynamically associated with each of the four REs. Each of the data sets were plotted as cumulative sums over time and fit with a single exponential equation. (**A**) Unbound dwell times (268) obtained with the GADD45 RE were plotted. The rate constant from the single exponential fit is 0.052 s^{-1} with 95% confidence interval of 0.051-0.054 s^{-1}. (**B**) Unbound dwell times (105) obtained with the p21 RE were plotted. The rate constant from the single exponential fit is 0.030 s^{-1} with 95% confidence interval of 0.029-0.031 s^{-1}. (**C**) Unbound dwell times (268) obtained with the MDM2 RE were plotted. The rate constant from the single exponential fit is 0.0237 s^{-1} with 95% confidence interval of 0.0235-0.0240 s^{-1}. (**D**) Unbound dwell times (297) obtained with the PUMA RE were plotted. The rate constant from the single exponential fit is 0.0169 s^{-1} with 95% confidence interval of 0.0166-0.0173 s^{-1}.

Figure 4. Under equilibrium conditions tetrameric p53 dissociated from each of the four REs in two kinetically distinct steps. Each of the data sets were plotted as cumulative sums over time and fit with a double exponential equation. The rate constants, 95% confidence intervals, and percentage of events contributing to each rate constant are shown in Table 1. (**A**) Bound dwell times (421) obtained with the GADD45 RE were plotted. The rate constants from the double exponential fit are 0.75 s^{-1} and 0.097 s^{-1}. (**B**) Bound dwell times (121) obtained with the p21 RE were plotted. The rate constants from the double exponential fit are 0.27 s^{-1} and 0.023 s^{-1}. (**C**) Bound dwell times (441) obtained with the MDM2 RE were plotted. The rate constants from the double exponential fit are 0.26 s^{-1} and 0.049 s^{-1}. (**D**) Bound dwell times (436) obtained with the

PUMA RE were plotted. The rate constants from the double exponential fit are 0.089 s^{-1} and 0.016 s^{-1}.

Figure 5. The dynamics of p53 tetramers interacting with p53 REs increases as DNA sequence becomes more similar to the consensus sequence. (**A**) The three measured rate constants are plotted for the four REs, which increase in similarity to consensus from left to right. The errors are 95% confidence intervals. (**B**) Kinetic model for the binding of p53 tetramers to an RE.

DNA	On rate constants			Off rate constants				Affinity
	$k_{on(obs)}$ (s-1)	95% CI	$t_{1/2}$ (s)	k_{off} (s-1)	95% CI	$t_{1/2}$ (s)	% of events	$K_{D(app)}$ (nM)
GADD45	0.052	0.051-0.054	13.3	0.75	0.71-0.79	0.92	36.1%	≤ 3.5
				0.097	0.094-0.100	7.2	63.9%	≤ 0.46
p21	0.03	0.029-0.031	23.1	0.27	0.25-0.29	2.6	52.9%	≤ 2.2
				0.023	0.020-0.025	30.1	47.1%	≤ 0.16
MDM2	0.0237	0.0235-0.0240	29.3	0.26	0.25-0.27	2.7	76.9%	≤ 2.6
				0.049	0.04-0.06	14.1	23.1%	≤ 0.50
PUMA	0.0169	0.0166-0.0173	41	0.089	0.085-0.095	7.8	66.1%	≤ 1.3
				0.016	0.013-0.019	43.3	33.9%	≤ 0.28

Table 1. The kinetic constants for tetrameric p53 binding to four native REs. The rate constants were derived from the fits of the data shown in Figures 3 and 4. Each 95% CI is the confidence interval of the rate constant obtained from the curve fit. Half-times were calculated using $t_{1/2} = \ln 2/k$. The % events was obtained from the double exponential curve fit and represents the distribution of p53/DNA complexes that dissociate with the corresponding rate constant. The apparent K_D values were calculated using the equation $K_D=k_{off}/k_{on}$, where k_{on} is the calculated second order rate constant determined using a concentration of 0.24 nM tetrameric p53.